International Journal of Chemical, Material and Environmental Research 2021, 8 (5): 01-10

Research article

INTERNATIONAL JOURNAL OF CHEMICAL, MATERIAL AND ENVIRONMENTAL RESEARCH

An International Open Free Access, Peer Reviewed Research Journal

ISSN 2410-5945
2021, Vol. 8, No. 5:
pg. 01-10

Determination of Cisaprid, Metoclopramide Hydrochloride

M. S. Kaiser[1*], Swagata Dutta[2]

[1]Directorate of Advisory, Extension and Research Services, Bangladesh University of Engineering and Technology, Dhaka-1000
[2]Institute of Appropriate Technology, Bangladesh University of Engineering and Technology, Dhaka-1000, Bangladesh

Abstract

The tribological performance of commercially used aluminium engine block and piston was evaluated at ambient conditions under dry and corrosive environment using a pin-on-disc with an applied load of 20 N at sliding velocity of 0.29 ms^{-1} and with varying sliding distance ranging from 260 m - 4200 m. The worn surfaces were characterized by optical microscope, SEM and EDX analyzer. The results showed that the nature of the wear rate was similar in both environments for both alloys which initially increases afterwards decreases to more or less a constant value. Moreover, for the block and piston alloys, the wear rate in corrosive environment was significantly higher than the dry condition. Due to the presence of Ni, higher percentage of Mg and lower percentage of Fe, the aluminium piston alloy showed higher wear performance than that of the block alloy.

Keywords: Aluminium-silicon alloys, engine block and piston, corrosion, wear, friction, SEM

1. Introduction

Aluminium-silicon (Al-Si) alloys have been commercially used to produce structural materials for automobile due to their high fluidity, low shrinkage in casting, high wear and corrosion resistance. To improve the weakness of aluminium alloys, Al-Si alloys including some other alloying elements such as Fe, Mg, Mn, Cu, Ni etc. are promising and developed by rapid solidification process. Because of their industrial importance, there is the necessity to study their corrosion and wear resistance and their mechanical properties [1, 2]. Corrosion normally occurs at a rate determined by the equilibrium between opposing electrochemical reactions [3]. Despite the excellent mechanical and physical properties of the Al-Si hypereutectic alloy, their corrosion resistance in aggressive environments is not yet well known. Some work has been carried out to evaluate the corrosion resistance of this alloy in alcoholic fuels [4, 5]. It has been suggested that corrosion of Al-Si alloy starts at the matrix/precipitate interface [6]. Wear is one of three most commonly encountered industrial problems, leading to the replacement of components and assemblies in engineering system, the others being fatigue and corrosion [3]. Because of the distinctive properties of Al-Si alloys, researchers become interested to study the properties of wear resistance of these alloys [7]. The mechanism of wear in these alloys involves the damage occurring on surface layers and subsurface, the deformation mechanism for this layer leads to the break-down of the second phase particles of more hardness (represent silicon) to small particles, which are distributed in subsurface region [1].

The purpose of this study is to investigate the wear behavior in corrosive environment of the commercially used Al-Si

Published online at www.ijcmer.org

engine block and piston alloys to put forward specific recommendations towards the tribological use of this alloy for local automobile spare parts manufacturers.

2. Materials and Methods

The materials used in the current study were commercial aluminium engine block and piston. The alloys were analyzed both by wet chemical and spectrochemical methods. The chemical compositions of the alloys are given in Table 1. The sample of 12 mm length and 5 mm diameter were machined from the engine block and piston for wear study by following ASTM Standard G99-05. The end surface (5 mm diameter) of the pin samples were polished using emery papers 1, 0, 2/0. Afterwards, the samples were polished in a fine grade wheel polisher. Later, the end surface was cleaned in running water. Finally, the samples were dried in acetone. Cast iron discs were used as the counter-body material. The hardness of the cast iron discs was around RC 50. One of the surfaces of the disc was grinded by surface grinding machine and cleaned with cotton.

The frictional and wear behaviors of the aluminium alloys were investigated in a pin-on disc type wear apparatus by following ASTM Standard G99-05. During the dry wear tests, the end surface of the pin samples were pressed against horizontal rotating cast iron disc. Applied load of 20 N was used throughout the test, which yielded nominal contact pressures of 1.4 MPa. The tests were conducted at the sliding speed of 0.29 ms^{-1} with varying sliding distances ranging from 260 m - 4200 m. The tests were carried out in ambient air (relative humidity 80%) under dry sliding condition (without lubrication). For corrosive wear test, 3.5% NaCl solution was used as the corrosive medium with all other parameters similar to dry wear test. Corrosive immersion test was used where the cast iron disc and the wear samples were immersed in 3.5% NaCl solution. At least four tests were done for each type of material. Wear rates were calculated from average values of weight-loss measurements. Wear rate was estimated by measuring the weight loss (ΔW) after each test. Care have been given after each test to avoid entrapment of wear debris. The wear rate was calculated using Equation 1.

$$W.R = \Delta W / S.D \qquad 1$$

where, $W.R$ is the wear rate, ΔW is weight loss and $S.D$ is the sliding distance.

Microstructural observation of the worn specimens were done carefully by using OPTIKA Microscope with a CCD camera (Model: OPTIKA) attached to PC at different magnifications and some selected photomicrographs were taken. The SEM investigation and EDX analysis were conducted by using a JEOL scanning electron microscope with an energy dispersive X-ray analyzer (Model: Link AN - 10000) attached.

Table 1. Chemical Composition of Al-Si Engine Block and Piston (wt %)

Alloy	**Si**	**Mg**	**Cu**	**Ni**	**Fe**	**Zn**	**Mn**	**Sn**	**Ti**	**Zr**	**Al**
Block	10.783	0.238	2.281	0.083	0.795	0.760	0.256	0.022	0.037	0.006	Balance
Piston	9.764	0.492	2.446	0.278	0.400	0.104	0.495	0.007	0.030	0.001	Balance

3. Results and discussion

Wear Test

Figure 1 and Figure 2 elucidate the variation of weight loss with the variation of sliding distance for both engine block and piston alloys at applied pressure of 1.4 MPa (Normal Load = 20 N) in dry and corrosive environment, respectively. Moreover, Figure 3 and Figure 4 depict the variation of wear rate with the variation of sliding distance for both engine block and piston alloys at applied pressure of 1.4 MPa (Normal Load = 20 N), respectively. Other parameters, such as sliding velocity (0.29 ms^{-1}), surface roughness (2 µm), and relative humidity (80%) are identical for these four figures. It can be seen from Figure 1 that, as the sliding distance increases the weight loss increases typically for both the alloys. However, the piston alloy shows relatively lower loss of weight. In case of weight loss in corrosive environment, the piston alloy shows little deviation from the dry condition. However, for block alloy, the weight loss is significantly higher than that observed in dry condition.

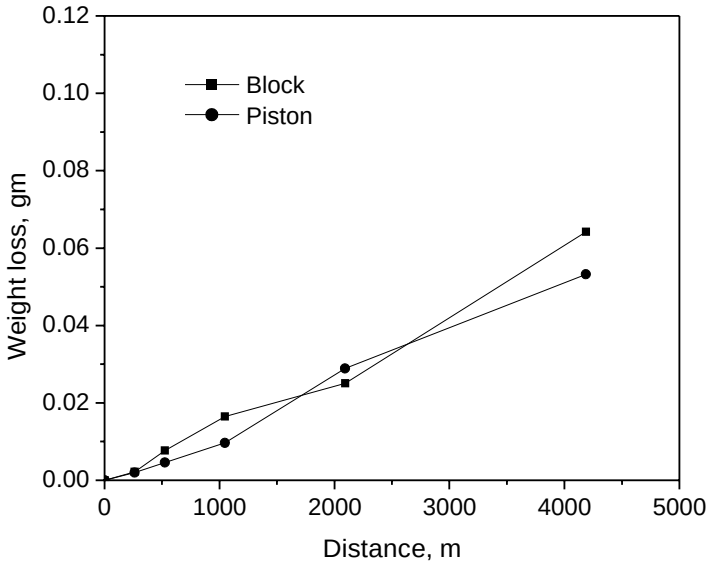

Figure 1. Variation of Weight Loss (gm) with the Variation of Sliding Distance (m) at Applied Pressure of 1.4 MPa (Load = 20 N) and Sliding Velocity 0.29 ms^{-1} in Dry Condition.

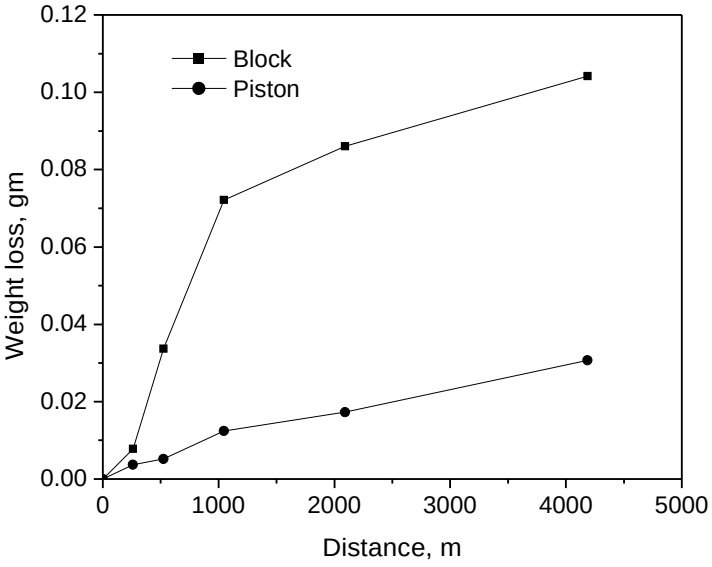

Figure 2. Variation of Weight Loss (gm) with the Variation of Sliding Distance (m) at Applied Pressure of 1.4 MPa (Load = 20 N) and Sliding Velocity 0.29 ms^{-1} in Corrosive Environment.

Figure 3 depicts that, the wear rate increases up to a certain point with sliding distance and afterwards attains a plateau for both block and piston alloys. However, the wear rate for piston alloy is lower than that of block alloy. In case of corrosive environment, the wear rate increases up to a certain point with sliding distance for both block and piston alloys where the wear rate of block was significantly higher than that of piston alloy. In both conditions, the piston alloy showed better wear performance. The result is due to the presence of Ni and higher percentage of Mg in the piston alloy as seen from Table 1. Ni forms Al_3Ni and presents a thin and homogeneous distribution of this intermetallic compound in the aluminium matrix. The Ni particles are distributed homogeneously in acicular forms inside the Al-Si matrix. The presence of this compound is found to increase the hardness and strength leading to lower wear rate. Mg, on the other hand, provides substantial strengthening and improvement of the work-hardening characteristics of aluminium alloys.

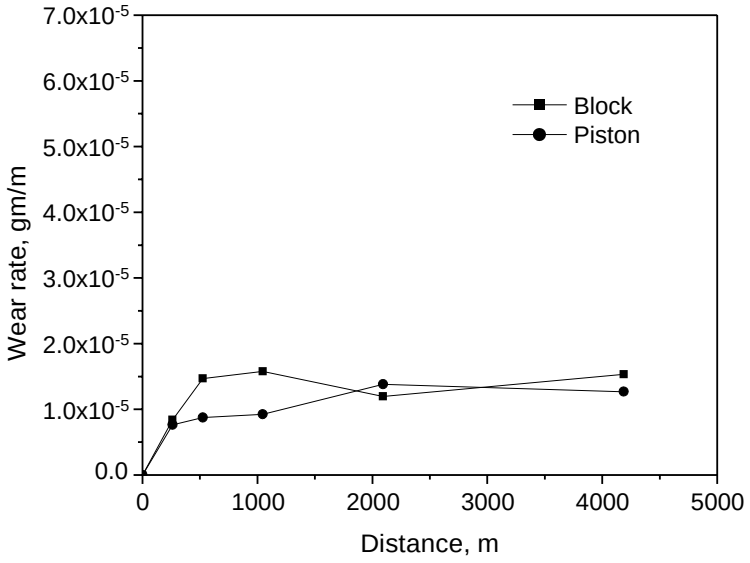

Figure 3. Variation of Wear Rate (gm/m) with the Variation of Sliding Distance (m) at Applied Pressure of 1.4 MPa (Load = 20 N) and Sliding Velocity 0.29 ms^{-1} in Dry Condition.

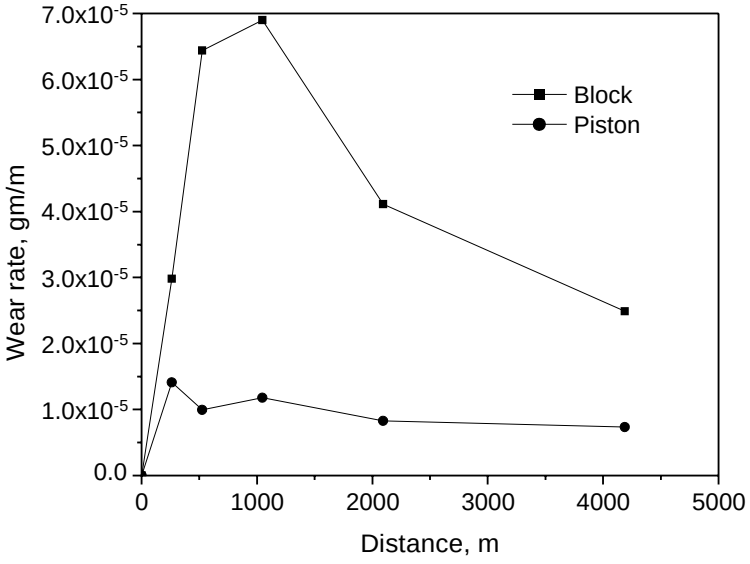

Figure 4. Variation of Wear Rate (gm/m) with the Variation of Sliding Distance (m) at Applied Pressure of 1.4 MPa (Load = 20 N) and Sliding Velocity 0.29 ms^{-1} in Corrosive Environment.

Silicon combines with Mg to form the hardening phase of Mg_2Si that provides substantial strengthening of the alloy. Mg content is beneficial to enhance the mechanical properties of the aluminium alloys and the abrasion resistance of the alloy due to uniformly distribution of hard particles and reduction of friction coefficient. The higher wear rate of block alloy can also be attributed to the fact that, it contains higher amount of Fe. The presence of Fe produces Al_3Fe precipitates which increase the susceptibility of the alloy to pitting corrosion [8, 9]. The behavior was due to the local increase of pH which is produced as a consequence of the reduction reaction of O_2 and is indicated as a possible cause of the formation of pits around the intermetallic compounds.

Optical Microscopic Observation

In this study of dry sliding wear of two Al-Si alloys against a cast iron counter-body, the wear was described as a mixed mode of elastic-plastic contact where Archard's law was obeyed. The applied pressure range investigated was 1.4 MPa.

This range of applied pressure was previously found to exhibit mild wear (MW) in these alloys [10].

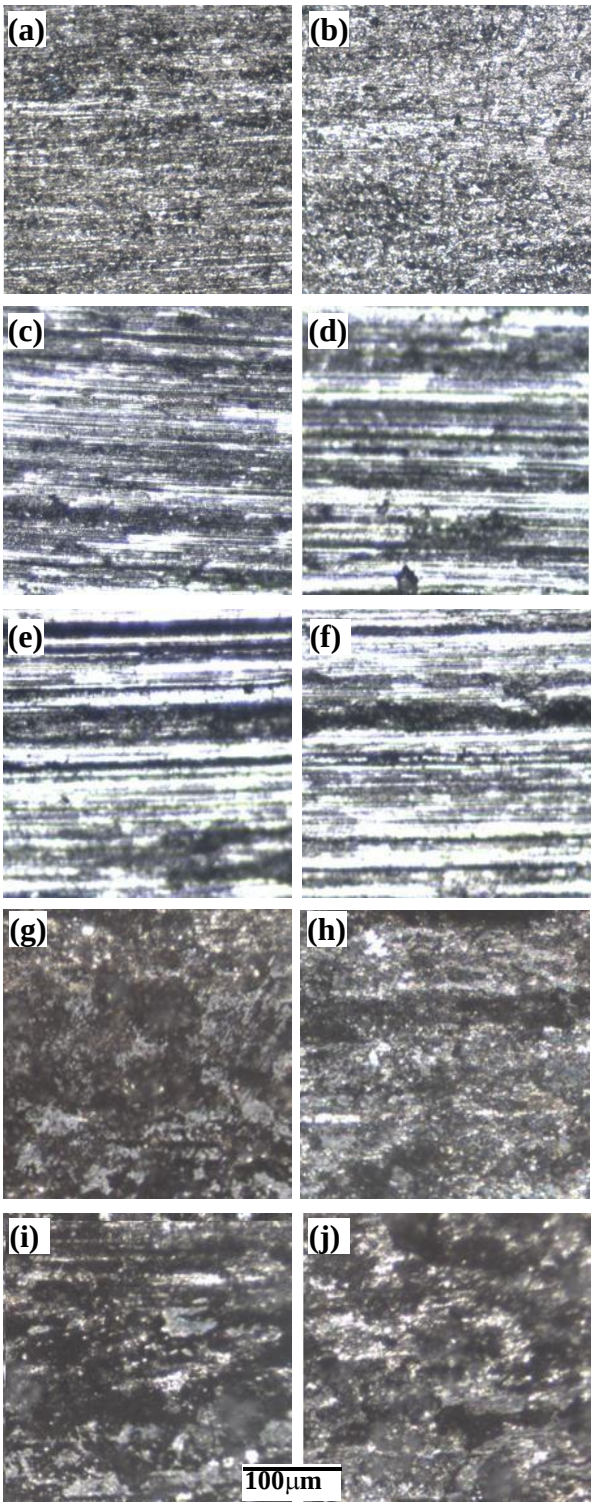

Figure 5. Optical Micrograph of Worn Surfaces before Wear a) Block, b) Piston, after Wear at Applied Pressure of 1.40 MPa for 15 min c) Block, d) Piston, for 4 hr e) Block, f) Piston, Corrosive Environment at Applied Pressure of 1.40 MPa for 15 min g) Block, h) Piston and for 4 hr i) Block, j) Piston.

In Figure 5 are presented the worn surfaces for both block and piston alloys at different environment and sliding distances. Figures 5a and 5b show the optical micrograph of polished aluminium engine block and piston, respectively. The samples have a microstructure characterized by an Al-rich dendritic matrix, α-Al phase and a eutectic mixture in the inter-

dendritic region formed by silicon particles, which are coarse and distributed in plate-like morrphology, set in an Al-rich phase [11]. In this type of image the precipitates of Al(Mn, Fe, Cu) are those that appear in the dark tone while those of Al(Si, Mg) appear in a lighter tone. Firstly, it can be observed that in both environment, for a given alloy and for an applied load of 20 N, as the sliding distance increases the wear marks becomes more visible and deep. In some portions of the investigated worn surface there are evidence of crater formation. From Figures 5c, 5d, 5e and 5f, it can be observed that, at dry condition and at all sliding distances, the wear marks in the worn surfaces of block and piston alloys are similar in nature. However, as the sliding distance increases the wear marks in both alloys becomes more visible and deep. At corrosive environment, no visible wear marks were observed in the worn surfaces of both alloys due to the presence of corrosion product. From Figures 5 g, 5h, 5i and 5j it can be seen that, the block alloy showed higher wear corrosion than that of piston alloy. No single wear mechanism can be attributed as the rate controlling mechanism throughout the mild wear regime. It was found that low loads and velocities produced sub-microscopic aluminium and iron particle debris which initially detach from the contact surfaces. This mechanically mixed phase predominantly consisted of aluminium oxide. The hardened aluminium oxide then facilitates the detachment of iron from the steel counter-face to produce the iron debris. This debris deposits on the surface and from time to time spall off, contributed to the wear.

SEM and EDX Observation

The SEM micrographs of as-received aluminium alloy engine block and piston are shown in Figures 6a and 6b, respectively. The microstructures consisted of mainly primary Al dendrite, eutectic Si, $Al_{15}(Fe, Mn)_3Si_2$, Mg_2Si and a few number of Fe-rich intermetallic phases on α-Al matrix in the inter-dendritic region. It can be seen that the eutectic Si phase is flake-like and acicular morphologies. A number of voids and cavities can be seen in the microstructure of the engine block alloy. From Table 1 it can be observed that the piston alloy contains significant amount of Ni. In case of piston alloy, two type of Al_3Ni phase are the plate-like and needle-like morphologies [12]. The Ni particles are distributed homogenously in acicular forms inside the Al-Si matrix without any cracks or voids between them. The Ni particles reacted with Al matrix forming Al_3Ni intermetalics. Addition of Ni particles decreases the Al-Si matrix grain size and eutectic dendritic arms but it increases the amount of α–phase.

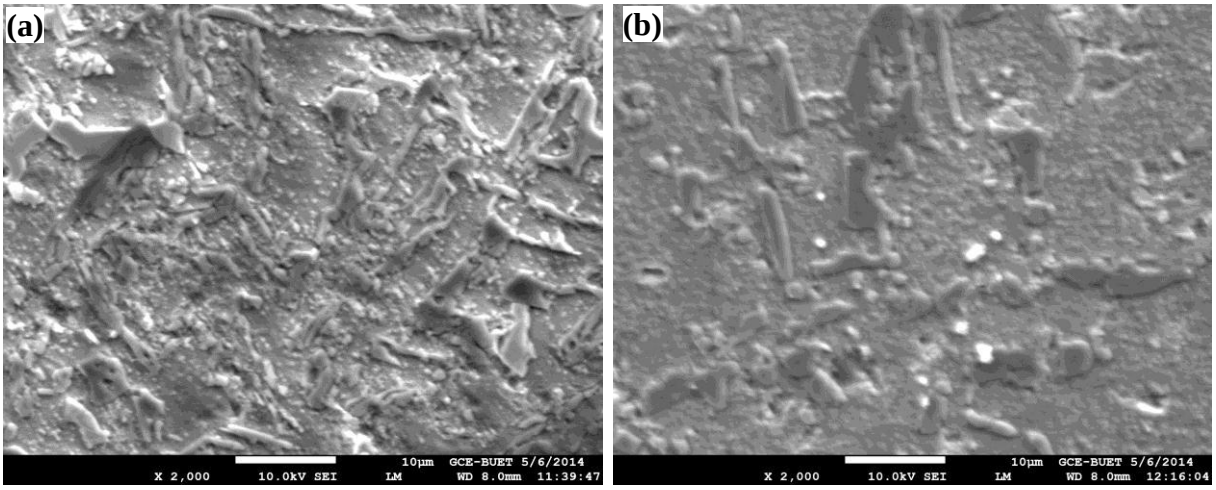

Figure 6. SEM Images of Aluminium Engine a) Block and b) Piston.

The SEM micrographs of worn surfaces of Al-Si block and piston alloys tested at 0.29 ms^{-1} under contact pressure 1.4 MPa in dry condition are shown in Figure 7. Sliding marks are observed on all the worn surfaces which are of typical ploughing action in comparatively soft metal. It is also seen that the depth and width of the sliding marks is higher for piston alloy. The presence of hemispherical pits is observed in both alloys. However, higher amount of pits were observed in block alloy than that of piston alloy (Figures 7a and7b). However, the distributions of pits were more uniform in case of piston alloy. The result is due to the presence of Ni which leads to better distribution of intermetallic [8].

The SEM image in the aluminium engine block after wear tested at 0.29 ms^{-1} under contact pressure 1.4 MPa in corrosive environment is shown in Figure 8, which indicates that the surface composes of two regions. One is covered with grass like corrosion products from which the mushrooms were formed and the other area is covered with a thin layer of corrosion products.

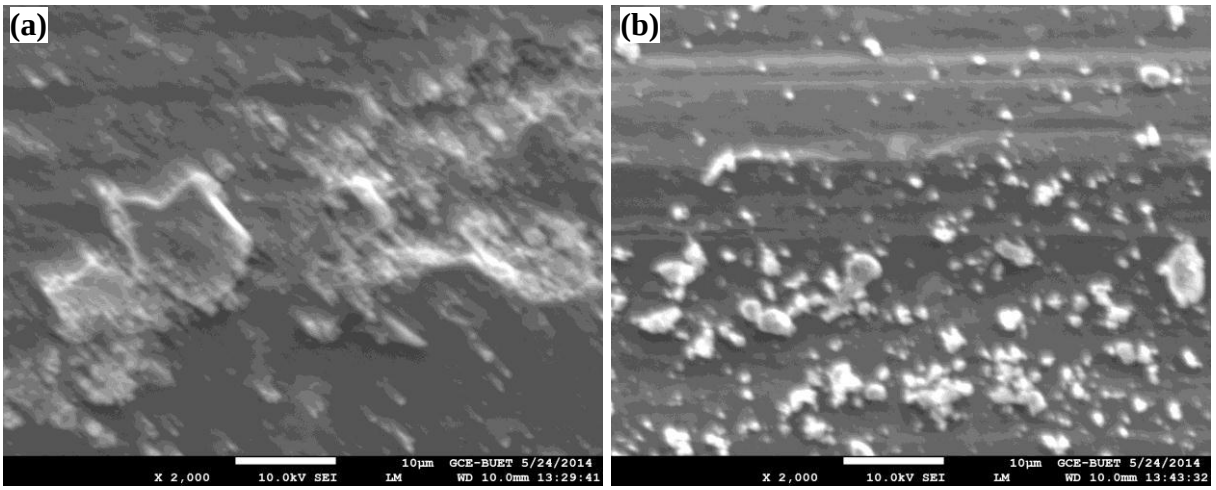

Figure 7. SEM Images of Aluminium Engine a) Block and b) Piston after Wear in Dry Condition at 1.4 MPa Applied Pressure and Sliding Distance of 4200m.

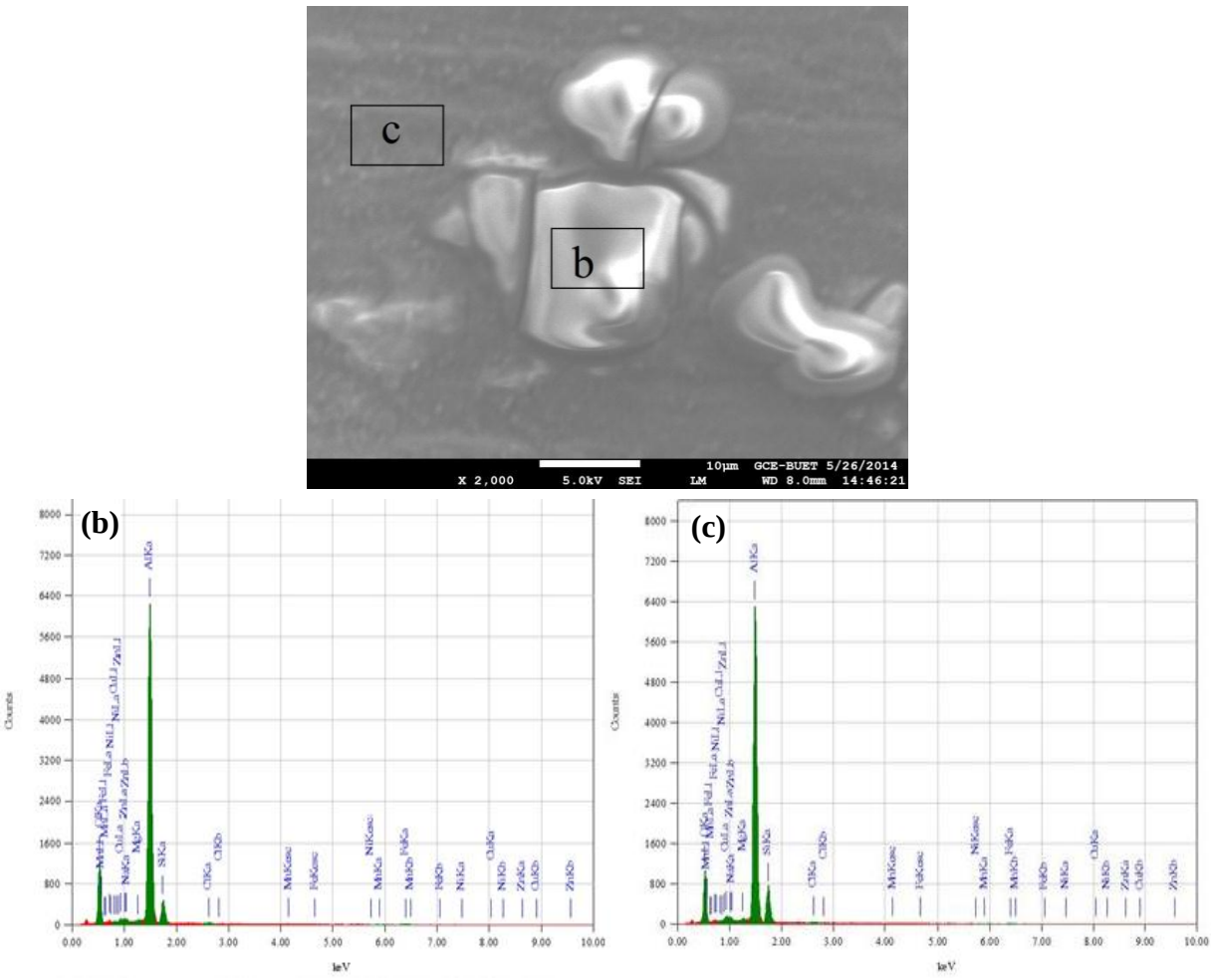

Figure 8. SEM Images and EDX of Engine Block after Wear in Corrosive Environment at 1.4 MPa Applied Pressure and Sliding Distance of 4200 m.

The corresponding EDX profile analyses for the selected square areas of the SEM are shown in Figures 8b and 8c. The weight percentage of elements found in white area were 25.34% O, 0.13% Na, 0.05% Mg, 62.81% Al, 7.29% Si, 0.31% Cl, 0.22% Mn, 2.35% Fe, 0.59% Cu and 0.92% Zn and in dark area were 22.46% O, 0.15% Mg, 62.42% Al, 11.58% Si, 0.48% Cl, 1.18% Fe, 0.77% Cu and 0.96% Zn.

Similarly, the SEM image in the aluminium piston of the surface after wear corrosion is shown in Figure 9. The corre-

sponding EDX profile analyses for the selected square areas of the SEM are shown in Figures 9b and 9c. The weight percentage of elements found in white area were 43.59% O, 0.30% Na, 0.20% Mg, 40.76% Al, 8.47% Si, 0.34% Cl, 0.81% Mn, 4.20% Fe, 0.53% Ni, 0.79% Cu and 0.01% Zn and in dark area were 52.52% O, 1.15% Na, 0.17% Mg, 40.16% Al, 2.46% Si, 1.33% Cl, 0.65% Mn, 0.85% Fe, 0.37% Ni and 0.35% Cu. In 3.5% NaCl solution, it can be observed that the sample has been discalced as a consequence of fracturing of the surface film. The surface oxide film was observed to develop at an early period and increased in area and in thickness with the passage of time [13].

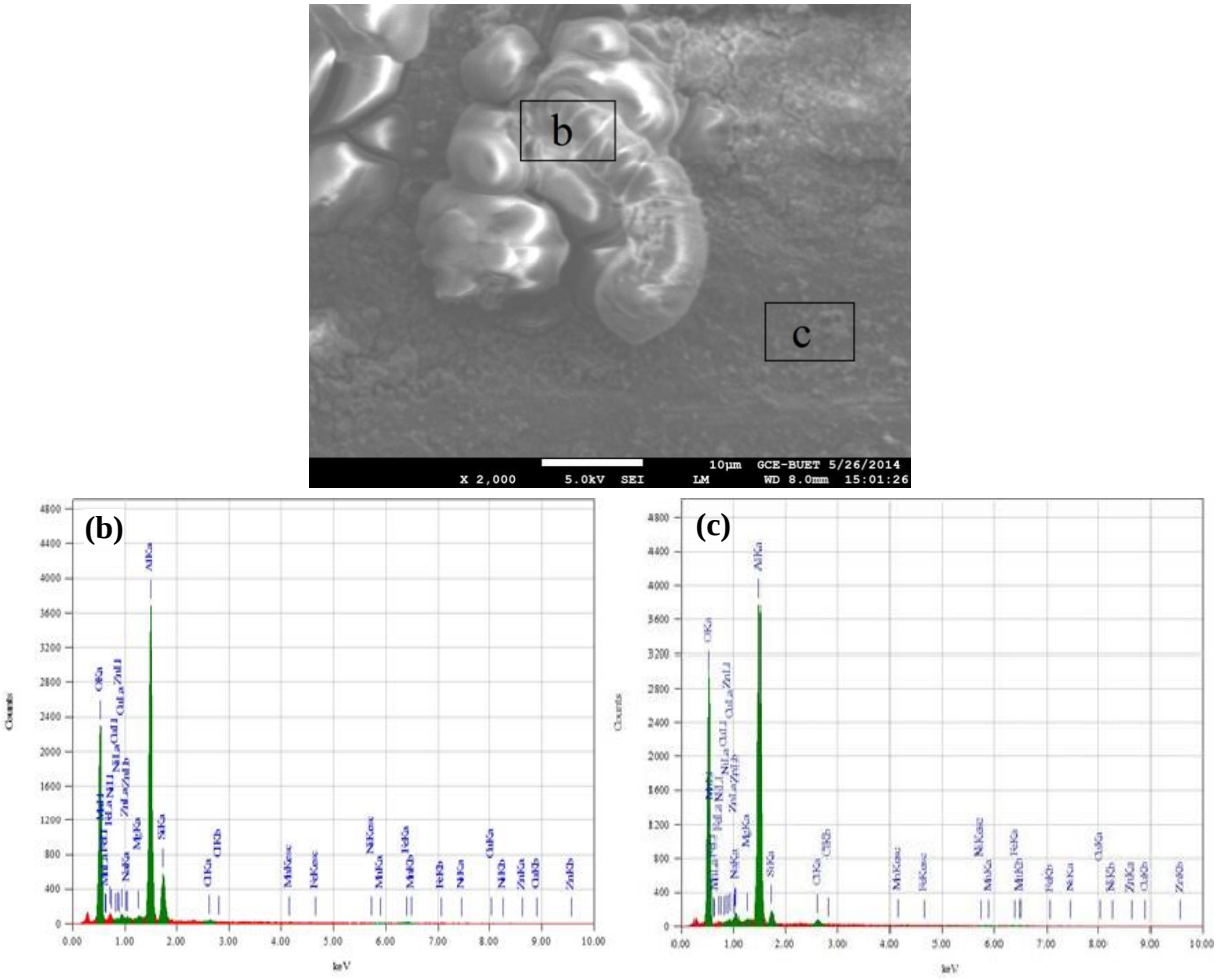

Figure 9. SEM Images and EDX of Piston after Wear in Corrosive Environment at 1.4 MPa Applied Pressure and Sliding Distance of 4200 m.

Figures 8 and 9 indicate that for both regions identified, the block alloy showed lower percentage of oxide content. This is due to the removal of oxide layer continuously in case of block alloy. However, for the piston alloy the rate of removal was found to be lower than that of the block alloy due to the presence of Ni, higher Mg and lower Fe. Ni and Mg increases the strength and harness leading to higher wear performance and Fe increases the susceptibility of the alloy towards pitting corrosion. These effects combined to produce the better wear performance of piston alloy.

4. Conclusions

The nature of the wear rate was similar in both environments for both alloys which initially increase and afterwards decreases to more or less a constant value. However, for the block and piston alloys, the wear rate in corrosive environment was significantly higher than the dry condition. The wear marks were not visible in corrosive environment. The hemispherical pits were found to be uniformly distributed in case of piston alloy. For the block alloy, the oxide content in corrosive wear was higher. Ni forms Al_3Ni and presents a thin and homogeneous distribution of this intermetallic compound in the aluminium matrix. Mg forms Mg_2Si that provides substantial strengthening of the alloy. Fe forms Al_3Fe precipitates which

increase the susceptibility of the alloys to pitting corrosion. Due to the presence of Ni, higher percentage of Mg and lower percentage of Fe, the aluminium piston alloy showed higher wear performance than that of block alloy.

ACKNOWLEDGEMENTS

This work is supported by CASR of Bangladesh University of Engineering and technology and is part of project “Studies of recrystallization, wear and corrosion behavior of aluminium piston and piston block”. Thanks to Department of Glass and Ceramics Engineering for providing the laboratory facilities.

REFERENCES

[1] Ye H., 2003. An overview of the development of Al-Si-Alloy based material for engine applications. JMEPEG, 12, 288-297.

[2] Kim Y.J., Kim J.C., 2011. Tensile property of Al-20% mass. Si alloys produced by a gas atomization process. RAMS, 28, 207-211.

[3] Jeffrey R.D., 1998. Metal Handbook. Second Edition, p. 488.

[4] Traldi S.M., Rossi J.L., Costa I., 2001. Corrosion of spray formed Al-Si-Cu alloy in ethanol automobile. Key Eng. Mater., 189, 352-357.

[5] Traldi S.M., Rossi J.L., Costa I., 2003. An electrochemical investigation of the corrosion behavior of Al-Si-Cu hypereutectic alloys in alcoholic environments. Revista de Metalurgia Supplemento S., 81, 86-90.

[6] Fontana M.G., Green N.D., 1997. Corrosion Engineering. 3rd Ed. Mc Graw Hill, pp. 454-457.

[7] Mohammed K.J., Dwarakadasa E.S., 1992. Dry sliding wear for Al-Si alloys at low bearing pressures. Mat. Sci. letters, 11, 421-423.

[8] Rana R.S., Purohit R., Das S., 2012. Reviews on the influences of alloying elements on the microstructure and mechanical properties of aluminium alloys and aluminium alloys composites. IIJSRP, 2, 1-7.

[9] Osorio W.R., Cheung N., Peixoto L.C., Garcia A., 2009. Corrosion resistance and mechanical properties of an Al 9wt%Si alloy treated by laser surface remelting. Int. J. Electrochem. Sci., 4, 820-831.

[10] Deuis R.L., Subramanian C., Yellup J.M., 1996. Abrasive wear of aluminium composites - A Review. Wear, 201, 132-144.

[11] Chaudhury S.K., Warke V., Shankar S., Apelian D., 2011. Localized recrystallization in cast Al-Si-Mg alloy during Solution heat treatment: Dilatometric and calorimetric studies. Met. Tran. 42A, 3160-3169.

[12] Lasa L., Rodrigues-Ibade J.M., 2003. Wear behaviour of eutectic andhypereutectic Al-Si-Cu-Mg casting alloys tested against a composite brake pad. Mater. Sci. Eng. A, 363, 193-202.

[13] Kaiser M.S., Dutta S., 2014. Comparison of corrosion behaviour of commercial aluminium engine block and piston in 3.5% NaCl solution. MSEJ, 1, 9-17.

Int. J. Chem. Mater. Environ. Res. 2021; 8 (5): 01-10